Journal of Climate Change, Vol. 9, No. 4 (2023), pp. 45-52.
DOI 10.3233/JCC230031

Reduction in the Strength of Agulhas Current During Quaternary: Planktic Foraminiferal Records for 1.2 Million Years from IODP Hole U-1474A

Vikram Pratap Singh*, Shivani Pathak and Rahul Dwivedi
Department of Geology, Indira Gandhi National Tribal University, Amarkantak, India
✉ vikram.singh@igntu.ac.in

Received October 5, 2023; revised and accepted October 28, 2023

Abstract: The Agulhas Current (AC) had been quite variable during the Quaternary Period, which not only impacted the Agulhas Leakage (AL) but also caused changes in the AMOC. To study the changes in the strength of AC, planktic foraminiferal census count and stable oxygen isotope data from the IODP Hole U-1474A were generated for the last 1.2 million years (My). We recorded significant variations in the abundance of climate-sensitive species, which were grouped according to their ecological preference as warm tropical-subtropical Agulhas Fauna (AF), temperate-subpolar Southern Ocean Fauna (SOF), stable oxygen isotope records and the Subtropical Front (STF) Index. The correlation of these records suggests that the strength of AC reduced during seven intervals during the last 1.2 My, in response to cooling climate, which led to the northward shift of STF. The studied interval was divided into three periods of MPT, MPT-MBE and post-MBE events. The AC was strongest after the Mid-Brunhes Event (0.43 Ma) as compared to the Mid-Pleistocene Transition (MPT) and post-MPT to MBE intervals.

Keywords: Agulhas current; Agulhas leakage; Planktic foraminifera; Sub tropical front; Oxygen isotope ratio.

Introduction

The AC is the largest western boundary current in the world oceans (Simon et al., 2013), carrying ~70 Sv water (Lutjeharms, 2006). It transports warm and saline water to the Atlantic Ocean via the AL and then returns to the Indian Ocean as the Agulhas Return Current (ARC) to become a part of the Southwest Indian Ocean subgyre (Gordon, 1986; Lutjeharms and Ansorge, 2001; Lutjeharms, 2006). The AC feeds the returning arm of the global ocean conveyor belt through the AL (Gordon et al., 1992; Beal et al., 2011), leading to a stronger Atlantic Meridional Overturning Circulation (AMOC) (Biastoch et al., 2009; Simon et al., 2013).

The main factors controlling the AL are the strength of the AC and the position of the STF (Beal et al., 2011). STF is an oceanic front that defines the southern extent of the Agulhas system (Cartagena-Sierra et al., 2021). It separates the subtropical water from the subantarctic water and its northward migration determines the displacement of Southern Hemisphere westerlies as well as the strength of the AC and AL (Bard and Rickaby, 2009). Several studies have suggested that the migration of the STF northward during the glacial period significantly reduced the AL (Flores et al., 1999; Bard and Rickaby, 2009; Beal et al., 2011; Caley et al., 2014). Bard and Rickaby (2009) demonstrated equatorward migration of the STF during the cold stadials, nearly shutting off the AC. The hydrographic variations in the AC alter the water mass properties and volume transport of the AL (Simon et al., 2013). The reduced AC, due to the northward migration of the STF in response to

*Corresponding Author

glacial climates could significantly lower the AL.

The AL and its impact on the AMOC in response to the quaternary glacial-interglacial climates have been well-studied over the last few decades using the planktic foraminifera (PF) as proxy (Rau et al., 2002; Peeters et al., 2004; Franzese et al., 2006; Rau et al., 2006; Bard and Rickaby, 2009; Franzese et al., 2009; Dickson et al., 2010; Martínez-Méndez et al., 2010; Caley et al., 2012; Simon et al., 2013; Nirmal et al., 2023). Latitudinal migration of STF during the glacial-interglacial periods has been considered an important factor impacting the AL and has been well documented using PF from the Cape Basin (Peeters et al., 2004) and western Indian Ocean (Caley et al., 2012, 2014; Nirmal et al., 2023).

A few high-resolution, multiproxy studies on the AC have been attempted, correlating its impact on AL in the Atlantic Ocean (Caley et al., 2011, 2012; Simon et al., 2013, 2015), but the studies to document the changes in the upstream AC over longer timescales are scanty.

Hutson (1980) reported reduced AC during the glacial intervals on the basis of the distribution of PF in the Recent sediments from the SW Indian Ocean. Peeters et al. (2004) reported enhanced AL at the end of the past five glacial periods using the PF records from the Cape Basin. Nirmal et al. (2023) inferred strengthened AL at the major glacial-interglacial transitions during the Pleistocene using the PF records.

In the present study, we attempt to document the changes in the strength of the AC during the last 1.2 My, using PF census and stable isotope records from the IODP Hole U-1474A.

Study Area

The study area, IODP Hole U-1474A (31013.00'S; 31032.71'E), located in the southwest Indian Ocean, is strongly affected by the AC (Hall et al., 2017). It is located correct ~40 south to ~4° South of the latitude where AC gets fully constituted (Figure 1). The core obtained from IODP Hole U-1474A comprises an undisturbed sedimentary sequence of ~200 m, consisting of a well-preserved PF assemblage (Hall et al., 2017). The location of the hole, along with the well-preserved fauna makes it an ideal site to examine the PF records to establish the paleoceanography of the AC during the last 1.2 My.

Materials and Methods

We processed 150 samples from the IODP Hole U-1474A using the wet-sieving method to extract PF. The >150 µm fraction of the PF was used for the census count studies. This fraction is most commonly used for generating the relative abundance data (Sinha et al., 2006). The species identification was done following the taxonomy of Kennett and Srinivasan (1983). The preservation of PF at U-1474A is very good with high species diversity, characterised by a

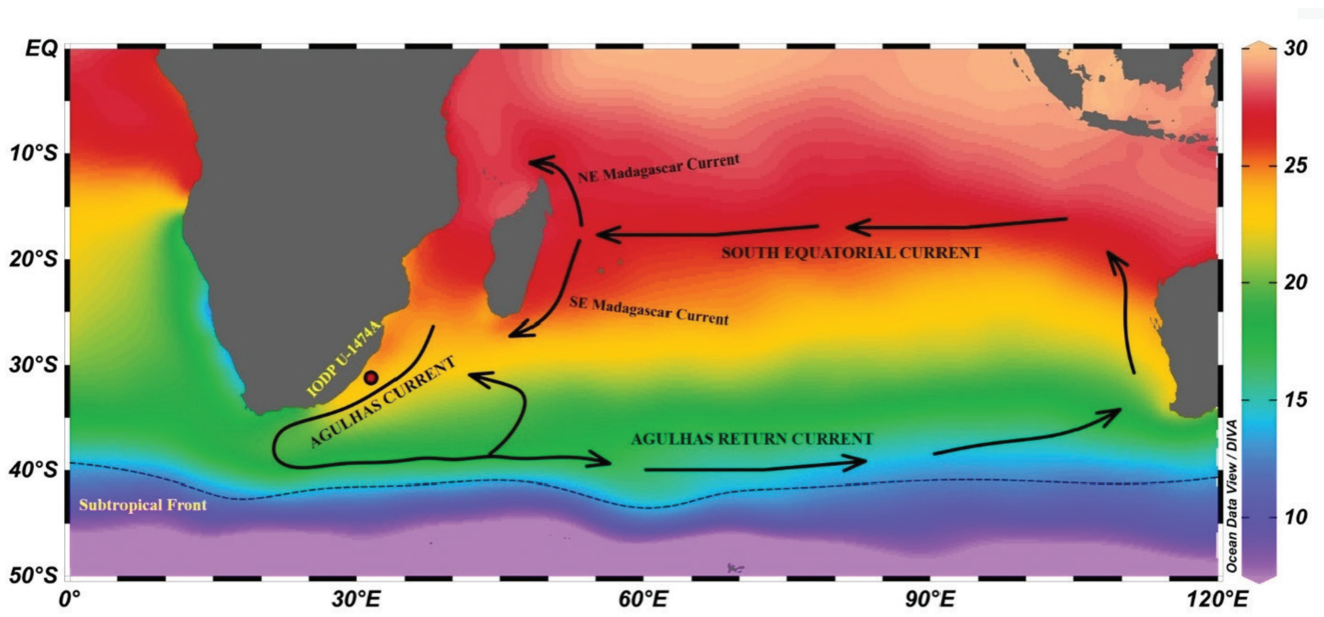

Figure 1: Modern circulation pattern and location of IODP Hole U-1474A.The underlying map of modern sea surface temperature was compiled with data from World Ocean Atlas 18 (Locarnini et al., 2018) and the ODV software version 5.6.3 (Schlitzer, 2022).

mixture of subtropical, temperate and subpolar forms. We created three groups on the basis of the ecological preference of PF (Bé and Hutson, 1977). Group 1, named Agulhas Fauna (AF) consisted of the warm, mixed-layer dwellers (Kennett and Srinivasan, 1983; Schiebel and Hemleben, 2017) *Globigerinoides (Gs.) ruber, Gs. triloba,* and *Gs. sacculifer*. Group 2, termed Southern Ocean Fauna (SOF) consisted of temperate and subpolar species (Kennett and Srinivasan, 1983; Schiebel and Hemleben, 2017) including *Globorotalia (Gr.) inflata, Gr. puncticulata,* and *Neogloboquadrina incompta*. Group 3, Upwelling Indicators (UI) included *Globigerina bulloides* and *Globigerinita glutinata,* which mark upwelling episodes and increase under fertility conditions (Sinha et al., 2006; Schiebel and Hemleben, 2017).

Stable oxygen isotope analysis was conducted on *Gs. ruber,* which is widely used for isotopic analysis of the surface water (Mohtadi et al., 2009). We used 4 to 5 ultrasonically cleaned specimens of *Gs. ruber* for the stable oxygen isotopic analysis in a Kiel IV Carbonate device and Thermo MAT 253 Plus isotopic ratio mass spectrometer device at IISER Kolkata. The results are reported relative to the Vienna Pee Dee Belemnite (VPDB). The oxygen isotope data is reported in δ notation relative to VPDB.

The chronology of the core was developed using the detailed magnetostratigraphy of IODP Hole U-1474A (Hall et al., 2017). Using the absolute ages of the paleomagnetic events (Ogg, 2020) recorded at Hole U-1474A and assuming a uniform sedimentation between recorded events, we calculated the age of each sample (Figure 2).

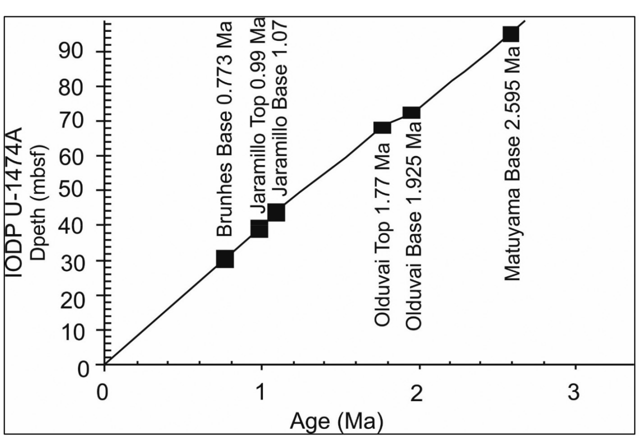

Figure 2: Age-depth plot of IODP Hole U-1474A. Paleomagnetic stratigraphy after Hall et al. (2017) and revised ages after Ogg (2020).

To identify the events of STF migration we calculated the STF Index following Peeters et al. (2004), using the relative abundance of three species, subtropical to transitional water dweller *Gr. truncatulinoides,* while the southern subtropical to subantarctic species *Gr. inflata* and *N. incompta*.

$$\text{STF Index} = \frac{Gr. truncatulinoides}{(Gr. truncatulinoides + Gr. inflata + N. incompta)}$$

The lower values of the STF Index mark the northward position of STF, while higher values indicate the southward position (Peeters et al., 2004).

The studied time period was divided into three intervals: (a) Mid Pleistocene Transition (MPT)- 1.2 to 0.7 Ma, (b) post-MPT to Mid-Brunhes Event (MBE)- 0.7 to 0.43 Ma, and (c) post-MBE- 0.43 Ma to Present.

Results

The PF assemblage at Hole U-1474A is a mixture of warm tropical-subtropical, temperate and subpolar species. Though the tropical-subtropical forms dominated during the last 1.2 My, the cold-water forms showed a significant rise several times, indicating a remarkable fluctuation in the climate-sensitive species.

The population of the AF shows significant variations during the last 1.2 My (Figure 3a). The overall abundance AF during the MPT was high between 1.2 and 1.0 Ma, after which it declined between 1.0 and 0.89 Ma, reaching a minimum of 8% at 0.9 My. It again increased by ~28% between 0.89 and 0.78 Ma, after which there was a sharp decline of 25% at the end of MPT. The post-MPT to MBE interval showed lower abundance as compared to the MPT. This interval began with a rise of 15% in AF from 0.7-0.57 Ma, following which, there was a 17% decline in the population from 0.57-0.48 Ma. This event was succeeded by a 25% increase in the population from 0.48-0.43 Ma. The MBE (0.43 Ma) showed the highest abundance with AF constituting ~38% of the total faunal component.

The post-MBE interval started with a sharp decline of 30% in AF*,* which continued up to 0.36 Ma. There were four events of significant rise in AF, 0.36-0.32 Ma, 0.27-0.22 Ma, and 0.17-0.09 Ma and 0.016-0.00025 Ma. All these events showed an increase of 15-25% in AF.

The relative abundance of the SOF witnessed significant changes during the studied interval (Figure 3b). The MPT witnessed two events of significant rise, from 1.0-0.89 Ma, and from 0.78-0.70 Ma, showing an increase of 43% and 31%, respectively. The post-MPT to MBE interval started with a 30% decline from 0.7-

0.57 Ma, followed by a 27% rise from 0.57-0.48 Ma. Following this increment, there was a decline till MBE, reached the lowest abundance of ~2%. The post-MBE interval witnessed a sharp rise in SOF from 0.43-0.36 Ma. At 0.42 Ma, the abundance was maximum to constitute 52% of the total faunal content. There were three more episodes of rise in the population, from 0.32-0.23 Ma, 0.22-0.17 Ma, and 0.09-0.016 Ma, which showed over 31% abundance of SOFG. The overall abundance of the SOF was the highest during the post-MBE interval.

The abundance of UI at Hole U-1474A (Figure 3c) during MPT increased during 1.2-1.1 Ma, 0.9-0.85 Ma and 0.79-0.71 Ma, with the highest abundance of 41%. It declined significantly between 1.1-0.9 Ma, and 0.71-0.7 Ma, when there was a 35% decrease. The post-MPT to MBE interval witnessed two events of high abundance of UI, between 0.70-0.63 Ma and 0.48-0.43 Ma, showing more than 15% rise. The UI abundance during the post-MBE interval was lower than the previous two intervals, except for one event of rise by 20% between 0.12 and 0.04 Ma.

The $\delta^{18}O_{Gs.\ ruber}$ showed significant variations during the three intervals (Figure 3d). There was a positive excursion of ~1.5‰ during MPT twice, between 1.15-9 Ma, and 0.84-0.73 Ma. The post-MPT to MBE interval showed two events of positive excursion in $\delta^{18}O$, between 0.71-0.67 My and 0.65-0.47 Ma. The post-MBE interval witnessed four events of positive excursion in $\delta^{18}O$, between 0.44-0.36 Ma, 0.33-0.23 Ma, 0.22-0.11 Ma and 0.08-0.01 Ma. All these events showed a cyclicity of approximately 100 ky, indicating the eccentricity-driven signals.

The STF Index (Figure 3e) started with the maximum value at the beginning of the MPT, after which this interval saw consistent lower values during this interval. The post-MPT to MBE interval also witnessed lower values, while the highest value of STF Index were attained during the post-MBE interval. The lowest STF Index value was seen close to the MBE at 0.47 Ma.

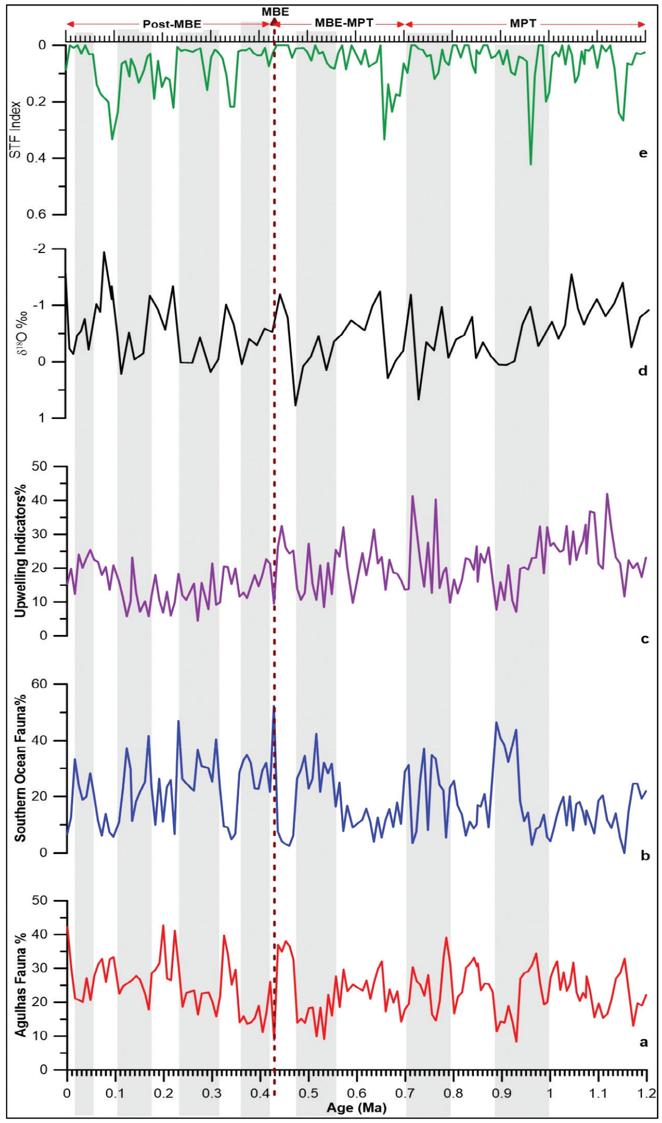

Figure 3: Correlation of the relative abundance of the PF groups with $\delta^{18}O_{Gs.\ ruber}$. The relative abundance of a. *Agulhas Fauna,* b. *Southern Ocean Fauna,* c. *Upwelling Indicators,* d. $\delta^{18}O_{Gs.\ ruber}$ and e. STF Index. The grey bars indicate the events of weakened AC, based on the PF census data. MPT- Mid-Pleistocene Transition; MBE-Mid-Brunhes Event.

Discussion

Given the location of Hole U-1474A, the PF census data must record the changes in the water mass, due to AC variations. The higher abundance of AF is indicative of stronger AC, while the rise in SOF marks a shift to cooler conditions due to reduced AC flow.

The seven events of increase of SOF (Figure 3) during the last 1.2 My reflect the periods of enhanced equatorward transport of cold waters. These events are also corroborated by a significant decline in the AF and positive excursion in the $\delta^{18}O$ values, which indicate a weakening of the AC. The lower STF Index values indicate northward migration of STF, which probably was the reason for the reduced AC.

The MPT began with warmer conditions as marked by a high AF population, followed by the onset of cooler conditions, depicted by a sharp rise in the SOF from 1.0 to 0.89 My. Nuber et al. (2021) have demonstrated cooling in the Indian Ocean, during the

MIS 22 (0.9 Ma), which probably was in response to the development of glacial conditions. At U-1474A, the cold conditions peaked at 0.9 Ma, showing the maximum abundance of SOF. The extremely low values of the STF Index, indicate the northward migration of the STF, thereby reducing the AC, allowing the intrusion of colder temperate waters to this site.

There was a return to warmer conditions between 0.89-0.78 Ma, with extremely low SOF and higher values of STF Index marking its retreat, probably in response to the end of the long-term cooling trend at 0.9 Ma (McClymont et al., 2013; Cartagena-Sierra et al., 2021). We infer this event as a strengthening of the AC.

Following this short event, the population of SOF again increased from 0.78-0.70 My, along with a significant rise in the UI, indicating enhanced upwelling. The upwelling could be in response to the latitudinal shift in the position of the southern hemisphere westerlies due to cooling (Bard and Rickaby, 2009). The low STF Index marks a northward migration of the STF. These evidences indicate reduced AC.

These two events of weakening of the AC were probably in response to the glacial climate, which led to the development of the first Northern Hemisphere continental-scale ice sheets at MIS 36 (~1.2 My) (Mudelsee and Stattegger, 1997), and the Antarctic Sea Ice waxing during MPT (Raymo et al., 2006).

The post-MPT to MBE interval began with extremely warm conditions, shown by a high abundance of AF, which also witnessed low SOF and southerly positioned STF. The UI showed variability in its abundance and recorded an overall decrease since the end of the MPT interval. It seems consistent with the southward migration of the STF, which caused the strengthening of the AC and return to warm conditions. This event was followed by an unprecedented rise in SOF from 0.57 to 0.47 Ma, marking an extremely cold event. The STF was consistently positioned northwards during this period, causing a significant weakening of the AC. This situation allowed the intrusion of cold, temperate waters into the U-1474A. The rise in the UI also indicates enhanced upwelling. This event approximates the MIS 12 (0.47 Ma), which has been reported as an exceptionally cool and productive glacial period (Bard and Rickaby, 2009), and has also been marked by the lowest abundance of ALF at ODP 1088B (Nirmal et al., 2023) and in Cape Basin (Peeters et al., 2004), indicating an extremely reduced AL. Caley et al. (2014) have identified this event from the Atlantic Ocean as the complete shutdown of the AL. These records mark an extremely weak AC at 0.47 Ma.

The interval from 0.47 to 0.43 Ma saw a sharp rise of AF along with significantly reduced SOF. The PI continued to decline, while the higher STF Index indicated southward migration of STF. The MBE approximates closely with the Termination V (Raymo, 1997) and has been reported to have experienced an enhanced AL (Peeters et al., 2004; Nirmal et al., 2023). We infer this event as a strengthening of the AC.

The post-MBE interval began with extremely cold conditions from 0.43-0.36 Ma, as indicated by a sharp increase in SOF, while AF declined significantly. The STF Index values were extremely low, marking its northerly position, with a fairly high UI abundance. The positive excursion in $\delta^{18}O$ values marked the weakest AC at the beginning of the post-MBE interval, which approximates MIS 10, recorded as the period of extremely low AL (Caley et al., 2014). The reduction in the strength of the AC could have been in response to the global cold climates associated with reduced AMOC ventilation and amplification of the northern ice sheets (Bard and Rickaby, 2009).

The end of this glacial event has been marked by a sharp rise in the population of AF between 0.36-0.32 Ma. The extremely low SOF, declining UI and higher STF Index point towards significantly stronger AC.

There were three more events of rise in SOF, from 0.32-0.23 Ma, 0.18-0.13 Ma and 0.09-0.016 Ma, which also show extremely low AF, lower STF Index and higher UI. The $\delta^{18}O$ values increase by~1.8‰ during these events, representing weaker AC.

There was an abrupt increase in the AF close to the end of these three events, which marked a stronger AC. These records suggest that the AC became significantly stronger, close to the glacial terminations. Peeters et al. (2004) have reported an abrupt increase in the ALF at the last five terminations, indicating vigorous exchange between the Indian and Atlantic oceans, marking enhanced AL. Our records suggest that the enhanced AL during the glacial terminations post-MBE was due to the enhanced AC, which could also have been one of the contributing factors for the terminations. The $\delta^{18}O$ values also showed a sharp decline in agreement with the strengthening of the AC.

The higher STF Index during the post-MBE interval indicated a consistent southerly position of the STF. The regularly declining UI, which was lowest during the post-MBE interval also supports our inference. The southward migration of the STF must have strengthened the AC during the post-MBE interval.

The rise in the SST along with salinity during the later part of glacial cycles has also been observed at IODP U-1476 (Nuber et al., 2021). The warming and salinification of the western Indian Ocean close to the end of glacial periods post-MBE, was a regional event due to pulses of warmer and saltier ITF waters entering the Indian Ocean (Holbourn et al., 2011). The higher overall abundance of AF at Hole U-1474A and the abundant ALF from ODP 1088B (Nirmal et al., 2023) and Cape Basin (Peeters et al., 2004) corroborate well with our interpretation of the strongest AC during the post-MBE interval, which also enhanced the AL. Haonan et al. (2021), based on the clay mineral records since MIS 12 from the IODP U-1474, have marked the glacial events as cold and dry, while interglacial events as warm and humid, which also indicate the stronger AC during the post-MBE interval. The stronger AC must have accentuated the AMOC and caused enhanced ventilation in the global oceans.

Conclusions

The PF census records from IODP Hole U-1474A, corroborated with $\delta^{18}O$ during the last 1.2 My reveal seven events of reduction in the strength of the AC. These events indicate that the AC severing was a major cause for the AL reduction during the last 1.2 My, as has been confirmed in several studies. The reduced AC flow is marked by a high relative abundance of SOFand a lower abundance of AF. During MPT the weakest AC was witnessed at 0.9 Ma, while the post-MPT-MBE interval was marked by the weakest AC at 0.47 My. The AC was overall stronger during the post-MBE as compared to the previous two intervals. The weaker AC was in response to the northward migration of the STF due to the cold global climates and Antarctic Sea Ice waxing, which significantly reduced the AC as well as AL.

Acknowledgements

We thank the NCPOR-IODP India for providing financial assistance for this work (Grant No.: NCPOR/IODP/E.3947/2021). RD thanks NCPOR for the financial support in the form of JRF. SP was financially supported by a fellowship from IGNTU. The IODP Hole U-1474A core samples were acquired by VPS from the IODP Kochi Core Centre Japan (request no. #85276IODP). VPS, SP and RD thank IGNTU for the lab facilities and logistic support.

References

Bard, E. and Rickaby, R.E.M., 2009. Migration of the subtropical front as a modulator of glacial climate. *Nature*, **460:** 382-383. 10.1038/nature08189

Bé, A.W.H. and Hutson, W.H., 1977. Ecology of planktonic foraminifera and biogeographic patterns of life and fossils assemblages in the Indian Ocean. *Micropalaentology*, **23(4):**369-414 https://doi.org/10.2307/1485406

Beal, L.M., De Ruijter, W.P.M., Biastoch, A. and Zahn, R., 2011. On the role of the Agulhas system in ocean circulation and climate. *Nature*, **472:** 429-436. 10.1038/nature09983

Biastoch, A., Böning, C.W., Schwarzkopf, F.U. and Lutjeharms, J.R.E., 2009. Increase in Agulhas leakage due to pole word shift of Southern Hemisphere Westerlies. *Nature*, **462(7272):** 495-498. 10.1038/nature08519

Caley, T., Kim, J.H., Malaizé, B., Giraudeau, J., Laepple, T.C., Caillon, N., Charlier, K., Rebaubier, H., Rossignol, P.E., Castañeda, I.S., Schouten, S. and Sinninghe Damsté, J.S., 2011. High-latitude obliquity as a dominant forcing in the Agulhas current system. Clim. of the Past, **7(4):** 1285-1296. https://doi.org/10.5194/cp-7-1285-2011

Caley, T., Giraudeau, J., Malaizé, B., Rossignol, L. and Pierre, C. 2012. Agulhas leakage as a key process in the modes of Quaternary climate changes. *Proc. Natl. Acad. Sci. U.S.A*., **109(18):** 6835-6839. https://doi.org/10.1073/pnas.1115545109

Caley, T., Peeters, F.J., Biastoc, A., Rossignol, L., Van Sebille, E., Durgadoo, J. and Malaizé, B., Giraudeau, J., Arthur, K. and Zahn, R., 2014. Quantitative estimate of the paleo–Agulhas leakage. *Geophysical Research Letters*, **41(4):** 1238-1246. https://doi.org/10.1002/2014GL059278

Cartagena-Sierra, A., Berke, M.A., Robinsin, R.S., Marcks, B., Castañeda, I.S., Starr, A., Hall, I.R., Hemming, S.R. and LeVay, L.J., 2021. Latitudinal migrations of the subtropical front at the Agulhas plateau through the mid-pleistocene transition. *Paleocean. Paleoclim.,* **36(7):** e2020PA004084. https://doi.org/10.1029/2020PA004084

Dickson, A.J., Leng M.J., Maslin, M.A., Sloane, H.J., Green, J., Bendle, J.A., McClymont, E.L. and Pancost, R.D., 2010. Atlantic overturning circulation and Agulhas leakage influences on southeast Atlantic upper ocean hydrography during marine isotope stage 11. *Paleoceanography*, **25:** PA3208. https://doi.org/10.1029/2009PA001830

Flores, J.A., Gersonde, R. and Sierro, F.J., 1999. Pleistocene fluctuations in the Agulhas current retroflection based on the calcareous plankton records. *Mar. Micropal*., **37:** 1-22. https://doi.org/10.1016/S0377-8398(99)00012-2

Franzese, A.M., Hemming, S.R., Goldstein, S.L., 2009. Use of strontium isotopes in detrital sediments to constrain the glacial position of the Agulhas Retroflection. J. Paleocean.,

paleoclim., **24(2)**. https://doi.org/10.1029/2008PA001706
Gordon, A.L., 1986. Interocean exchange of thermocline water. *J. Geophys. Res.:Oceans*, **91(C4):** 5037-5046. https://doi.org/10.1029/JC091iC04p05037
Gordon, A.L., Weiss, R.F., Smethie Jr., W.M. and Warner, M.J., 1992. Thermocline and intermediate water communication between the South Atlantic and Indian Oceans. *J. Geophys, Res.: Oceans*, **97:** 7223-7240 https://doi.org/10.1029/92JC00485
Hall, I.R., Hemming, S.R., LeVay, L.J., and the Expedition 361 Scientists, 2017. Proceedings of the International Ocean Discovery Program Volume 361. 10.14379/iodp.proc.361.103.2017
Haonan, S., Yongcong, Z., Xibin, H., Bingyao, H.U., Feijiang, L., 2021. Provenance and climatic changes of the Natal Valley, Southeastern Africa since MIS 12: The clay mineral records from Hole U1474A, IODP 361. *Mar. Geol., Quat. Geol.,* **41(4):** 142-156. DOI:10.16562/j.cnki.0256-1492.2021042001
Hilbrecht, H., 1996. Extant planktic foraminifera and the physical environment in the Atlantic and Indian Oceans.- MitteilungenausdemGeologischenInstitut der Eidgen. Technischen Hochschule und der Universität Zürich, Neue Folge. 300, 93.
Holbourn, A., Kuhnt, W., Xu, J., 2011. Indonesian Throughflow variability during the last 140 ka: The Timor Sea outflow. *J. Geological Society, London, Special Publications*, **355(1):** 283-303.10.1144/SP355.14
Hutson, W.H.,1980. The Agulhas current during the late Pleistocene: Analysis of modern faunal analogs. *J. Science*, 207(4426): 64-66. https://doi.org/10.1126/science.207.4426.64
Kennett, J.P. and Srinivasan, M.S., 1983. Neogene Planktonic Foraminifera, A Phylogenetic Atlas: Hutchinson Ross Pub. Co., Stroudsburg, Pennsylvania.
Locarini R.A., Mishonov, A.V., Baranova O.K., Boyer, T.P., Zweng, M.M., Garcia, H.E., Reagan, J.R., Seidov, D., Weathers. K.W., Paver, C.R. and Smolyar, I.V., 2018. World Ocean Atlas 2018, Volume 1: Temperature. NOAA Atlas NESDIS 81, 52. https://archimer.ifremer.fr/doc/00651/76338/
Lutjeharms, J.R.E and Ansorge, I.J., 2001. The Agulhas Return Current. *Jour. Marine System*s, **30:** 115-138. https://doi.org/10.1016/S0924-7963(01)00041-0
Lutjeharms, J.R.E, 2006. The Agulhas Current. Springer, New York.
Martínez-Méndez, G., Zahn, R., Hall, I. R., Peeters, F.J.C., Pena, L.D., Cacho, I., and Negre, C., 2010. Contrasting multi-proxy reconstructions of surface ocean hydrography in the Agulhas Corridor and implications for the Agulhas Leakage during the last 345,000 years. *Paleoceanography*, **25:** PA4227, https://doi.org/10.1029/2009PA001879
McClymont, E.L., Sosdian, S.M., Rosell-Melé, A. and Rosenthal, Y., 2013. Pleistocene sea-surface temperature evolution: Early cooling, delayed glacial intensification, and implications for the mid-Pleistocene climate transition. *Earth-Science Reviews*, **123:** 173-193. https://doi.org/10.1016/j.earscirev.2013.04.006
Mohtadi, M., Steinke, S., Groeneveld, J., Fink, H.G., Rixen, T., Hebbeln, D., Donner, B. and Herunadi, B., 2009. Low-latitude control on seasonal and interannual changes in planktonic foraminiferal flux and shell geochemistry off south Java: A sediment trap study. *Paleoceanography*, **24:** PA1201. https://doi.org/10.1029/2008PA001636
Morard, R., Quillévéré, F., Douady, C.J., de Vargas, C., de Garidel-Thoron, T. and Escarguel, G., 2011. Worldwide genotyping in the planktonic foraminifer *Globoconella inflata*: implications for life history and paleoceanography. *PLOS One*, **6(10):** e26665. https://doi.org/10.1371/journal.pone.0026665
Mudelsee, M. and Stattegger, K., 1997. Exploring the structure of the mid-Pleistocene revolution with advanced methods of time-series analysis. *J. Geol Rundsch*, **86:** 499-511. https://doi.org/10.1007/s005310050157
Naidu, P.D. and Malmgren, B.A., 1996. A high-resolution record of late quaternary upwelling along the Oman Margin, Arabian Sea based on planktonic foraminifera. *J. Paleoceanography*, **11(1):** 129-140. https://doi.org/10.1029/95PA03198
Nirmal, B., Mohan, K., Tripati, A., Christensen, B.A., Mortyn, P.G., De Vleeschouwer, D., Prakasam, M. and Saravanan, K., 2023. Agulhas leakage extension and its influences on South Atlantic surface water hydrography during the Pleistocene. *Palaeogeo. Palaeoclim. Palaeoeco.*, **615(7253):** 111447 10.1016/j.palaeo.2023.111447
Nuber, S., Rae, J., Andersen, M., Zhang, X., de Boer, B., Dumont, M., Sun, Y., Mithan, H., Hall, I. and Barker, S., 2021. Sea Level controls on Agulhas Leakage Salinity and the Atlantic Overturning Circulation, 05 November 2021, PREPRINT (Version 1) available at Research Square [https://doi.org/10.21203/rs.3.rs-1038170/v1]
Ogg, J.G., 2020. Geomagnetic Polarity Time Scale. *In:* Gradstein, F.M., Ogg, J.G., Schmitz, M.D. and Ogg, G.M. (eds.). Geologic Time Scale 2020. Elsevier, pp. 159-192. https://doi.org/10.1016/B978-0-12-824360-2.00005-X
Peeters, F.J.C., Acheson, R., Brummer, G.J.A., de Ruijter, W.P.M., Schneider, R.R., Ganssen, G.M., Ufkes, E., and Kroon, D. 2004. Vigorous exchange between the Indian and Atlantic Oceans at the end of the past five glacial periods. *Nature*, **430(7000):** 661-665. 10.1038/nature02785
Rau, A.J., Rogers, J. and Chen, M.-T., 2006. Late Quaternary palaeoceanographic record in giant piston cores off South Africa, possibly including evidence of neotectonism. *J. Quaternary International*, **148(1):** 65-77. https://doi.org/10.1016/j.quaint.2005.11.007
Raymo, M.E., 1997. The timing of major climate transitions. *Paleoceanography*, **12(4):** 577-585.

Raymo, M.E., Lisiecki, L.E. and Nisancioglu, K.H., 2006. Plio-Pleistocene ice volume, Antarctic climate, and the global δ18O record. *Science*, **313(5786):** 492-495. https://doi.org/10.1126/science.1123296

Reynolds, L. and Thunell, R.C., 1985. Seasonal succession of planktonic Foraminifera in the subpolar North Pacific. *J Foram. Res*., **15:** 282-301. https://doi.org/10.2113/gsjfr.15.4.282

Schiebel, R. and Hemleben, C., 2000. Interannual variability of planktic foraminiferal populations and test flux in the eastern North Atlantic Ocean (JGOFS). *Deep Sea Research Part II: Topical Studies in Oceanography*, **47(9-11):** 1809-1852. https://doi.org/10.1016/S0967-0645(00)00008-4

Schiebel, R. and Hemleben, C., 2017. Planktic Foraminifers in the Modern Ocean. Springer-Verlag Berlin Heidelberg. 10.1007/978-3-662-50297-6

Schlitzer, R., 2022. Ocean Data View [Software]. Available from http://odv.awi.de.

Simon, M.H., Gong, X., Hall, I.R., Ziegler, M., Barker, S., Knorr, G., van der Meer, M.T.J., Kasper, S. and Schouten, S., 2015. Salt exchange in the Indian-Atlantic Ocean Gateway since the last glacial maximum: A compensating effect between Agulhas current changes and salinity variations? *Paleoceanography and Paleoclimatology*, **30:** 1318-1327. https://doi.org/10.1002/2015PA002842

Simon, M.H., Arthur, K.L., Hall, I.R., Peeters, F.J.C., Loveday, B.R., Barker, S., Ziegler, M. and Zahn, R., 2013. Millennial-scale Agulhas current variability and its implications for salt-leakage through the Indian-Atlantic Ocean Gateway. *J. Earth Planet. Sc. Lett*., **383:** 101-112. https://doi.org/10.1016/j.epsl.2013.09.035

Sinha, D.K., Singh, A.K. and Tiwari, M., 2006. Paleoceanographic and Paleoclimatic history of ODP site 763A (Exmouth Plateau). Southwest Indian Ocean: 2.2 Ma records of planktic foraminifera. *Current Science*, **90(10):** 1363-1369.https://doi.org/10.2113/gsjfr.52.4.248